REPORT DOCUMENTATION PAGE

Public reporting burden for this collection of information is estimated to average 1 hour per response, including the time for reviewing instructions, searching existing data sources, gathering and maintaining the data needed, and completing and reviewing the collection of information. Send comments regarding this burden estimate or any other aspect of this collection of information, including suggestions for reducing this burden, to Washington Headquarters Services, Directorate for Information Operations and Reports, 1215 Jefferson Davis Highway, Suite 1204, Arlington, VA 22202-4302, and to the Office of Management and Budget, Paperwork Reduction Project (0704-0188), Washington, DC 20503.

1. AGENCY USE ONLY (Leave blank)	2. REPORT DATE 9/5/96	3. REPORT TYPE AND DATES COVERED Interim; 4/10/96-9/30/96

4. TITLE AND SUBTITLE	5. FUNDING NUMBERS
Moving target detection and motion estimation in foliage using along track monopulse synthetic aperture radar imaging	N00014-96-1-0586

6. AUTHOR(S)

Mehrdad Soumekh

7. PERFORMING ORGANIZATION NAME(S) AND ADDRESS(ES)	8. PERFORMING ORGANIZATION REPORT NUMBER
Research Foundation of SUNY-Buffalo Office of Sponsored Programs Administration The UB Commons, Suite 211, 520 Lee Entrance Amherst, NY 14228-2567	

9. SPONSORING/MONITORING AGENCY NAME(S) AND ADDRESS(ES)	10. SPONSORING/MONITORING AGENCY REPORT NUMBER
Office of Naval Research Regional Office Boston 495 Summer Street, Room 103 Boston, MA 02210-2109	

11. SUPPLEMENTARY NOTES

12a. DISTRIBUTION/AVAILABILITY STATEMENT	12b. DISTRIBUTION CODE
Approved for public release.	

13. ABSTRACT (Maximum 200 words)

A system model for the effect of uncalibrated monostatic and bistatic radars via gain and phase functions which vary with the radars aspect angles and the radar frequency, and the resultant degradation in monopulse SAR images and their difference which is used for moving target detection, is developed. A signal subspace processing of monopulse SAR images and a signal subspace difference image for moving target detection, which is not sensitive to the unknown gain and phase error functions of the uncalibrated radars, are developed. Numerical results are provided.

14. SUBJECT TERMS		15. NUMBER OF PAGES 25
Along-tarck monopulse SAR; uncalibrated monopulse radars; signal subspace processing.		16. PRICE CODE

17. SECURITY CLASSIFICATION OF REPORT	18. SECURITY CLASSIFICATION OF THIS PAGE	19. SECURITY CLASSIFICATION OF ABSTRACT	20. LIMITATION OF ABSTRACT
Unclassified	Unclassified	Unclassified	

Progress Report for:

CONTRACT N00014-96-1-0586

MOVING TARGET DETECTION AND MOTION ESTIMATION IN FOLIAGE USING ALONG TRACK MONOPULSE SYNTHETIC APERTURE RADAR IMAGING

Submitted to:

Office of Naval Research
Program Officer William J. Miceli, ONR 3131
Ballston Centre Tower One
800 North Quincy Street
Arlington, VA 22217-5660

Administrative Grants Officer
Office of Naval Research Regional Office Boston
495 Summer Street, Room 103
Boston, MA 02210-2109

Director, Naval Research Laboratory
Attn: Code 2627
4555 Overlook Drive
Washingon, DC 20375-5326

Defense Technical Information Center
8725 John J. Kingman Road
STE 0944
Ft. Belvoir, VA 22060-6218

Distribution Statement:

Approved for public release.

Project Director:

Mehrdad Soumekh
Department of Electrical & Computer Engineering
State University of New York at Buffalo
Amherst, New York 14260
Phone: (716) 645-2422, extension 2138
Fax: (716) 645-3656
Email: msoum@eng.buffalo.edu
http://www.acsu.buffalo.edu/~msoum

i

CONTENTS

Progress Report:

MOVING TARGET DETECTION AND MOTION ESTIMATION IN FOLIAGE USING ALONG TRACK MONOPULSE SYNTHETIC APERTURE RADAR IMAGING

Mehrdad Soumekh
Department of Electrical & Computer Engineering
State University of New York at Buffalo
Amherst, New York 14260

1a. Overview

This document describes the progress on the work performed for "Moving Target Detection and Motion Estimation in Foliage Using Along Track Monopulse Synthetic Aperture Radar Imaging," under Contract N00014-96-1-0586 for the Office of Naval Research during the first six months of this contract (4/10/96 - 9/30/96).

The scope of the tasks for this period included the following:

i. Two-dimensional system and signal modeling of the effect of **uncalibrated** monostatic and bistatic radars via gain and phase error functions which vary with the radars aspect angles and the radar frequency, and the resultant degradation in monopulse SAR images and their difference which is used for moving target detection;

ii. Developing a **signal subspace** processing of monopulse SAR images and a signal subspace difference image for moving target detection which is not sensitive to the unknown gain and phase error functions of the uncalibrated radars.

This report includes the theoretical derivation of the gain and phase error functions effect in monopulse SAR images. The signal subspace modeling and processing of monopulse SAR images, and constructing the signal subspace difference statistic are described. Numerical results are provided.

1b. Publications

The work has produced the following journal article which would contain a note on the support from the Office of Naval Research under Contract N00014-96-1-0586:

M. Soumekh, "Moving target detection in foliage using along track monopulse synthetic aperture radar imaging," accepted for publication in *IEEE Transactions on Image Processing*.

1

2. Background

The along track monopulse SAR imaging system utilizes two radars for its data collection. One radar, Radar 1, is used as a transmitter as well as a monostatic receiver. The other radar, Radar 2, is used only as a bistatic receiver. In our original proposal and [1], we documented a signal processing algorithm of the two monostatic and bistatic databases of the along track monopulse SAR system to obtain two **coherently** identical SAR images of the stationary targets in the scene. While the stationary targets appear the same in the monostatic and bistatic SAR images, however, the same is not true for moving targets.

This fact is the basis for developing a static, which we refer to as the difference image, for moving target detection. If we denote the monostatic SAR image by $f_m(x, y)$ and the bistatic image by $f_b(x, y)$, the difference image for moving target detection is defined via the following:

$$f_d(x, y) = f_b(x, y) - f_m(x, y). \tag{1}$$

Figures 1a-c show this for a SAR scene in which the two radars are fully calibrated. [1] This example corresponds to a realistic FOPEN SAR database which is injected with the simulated signatures of four moving targets. The parameters of this SAR scene are outlined in our original proposal and [1]. Figures 1a and 1b, respectively, show the monostatic and bistatic SAR images of the target area which contain both foliage and moving targets. Figure 1c is the difference image which shows the signatures of the moving targets; the differencing operation has removed the signature of the stationary targets (foliage).

3. Effect of Uncalibrated Radars in Monopulse SAR Imaging

As we mentioned earlier, the result in Figure 1c is obtained with two radars which are fully calibrated; i.e., there is no relative gain and phase ambiguity in the data collected by the two radars. This idealistic scenario, however, is never encountered in practice. In a realistic monopulse SAR system, the two radars exhibit different amplitude patterns (phase as well as gain) which vary with the radar frequency and the radar position (i.e., the slow-time). Moreover, these amplitude patterns vary from one pulse transmission to another due to heat and other uncontrollable natural factors which affect the internal circuitry of the two radars. These subtle changes of the radars amplitude pattern are difficult to be detected and tracked, and are unknown to the user.

To develop a theoretical model for the undesirable variations of the amplitude pattern of uncalibrated monopulse radars and their effect in the difference image (for moving

---

[1] Figures are attached to the end of this report.

target detection), we begin with the signal model for the monostatic and bistatic SAR measurements. We denote the transmit-receive amplitude pattern of the monostatic radar in the spatial (x, y) domain by $a_m(x, y - u, \omega)$ where $(0, u)$ is the radar position on the synthetic aperture and ω is the radar (fast-time) frequency [2]. Thus, the monostatic SAR signal for a stationary unit reflector [2] at (x_n, y_n) is [2]

$$a_m(x_n, y_n - u, \omega) \; \exp\left[j2k\sqrt{x_n^2 + (y_n - u)^2}\right], \tag{2}$$

where $k = \omega/c$ is the wavenumber.

We define the following transformation of the amplitude pattern

$$A_m[2k \sin \theta_n(u), \omega] = a_m(x_n, y_n - u, \omega), \tag{3}$$

where

$$\theta_n(u) \equiv \arctan(\frac{y_n - u}{x_n}), \tag{4}$$

is the target's aspect angle when the radar is located at $(0, u)$. (See the discussion on the Fourier properties of the SAR's AM-PM signal in [2, Appendix] for a physical interpretation of (3).) Using the wavefront reconstruction algorithm for stripmap SAR [2], it can be shown that the Fourier transform of the monostatic SAR signal of (2) with respect to u (slow-time) yields the following target function in the spatial frequency domain:

$$F_m(k_x, k_y) = A_m(k_u, \omega) \; \exp(jk_x x_n + jk_y y_n), \tag{5}$$

where k_u is the spatial frequency domain for u, and

$$\begin{aligned} k_x &\equiv \sqrt{4k^2 - k_u^2} \\ k_y &\equiv k_u \end{aligned} \tag{6}$$

The spatial domain monostatic SAR image $f_m(x, y)$ is obtained via the two-dimensional inverse Fourier transform of $F_m(k_x, k_y)$.

A similar analysis can be performed for the bistatic measurement. Suppose the transmit-receive amplitude pattern of the bistatic scenario is $a_b(x, y - u, \omega)$. Then, after the phase compensation to convert bistatic SAR data to the equivalent monostatic

---

[2] One could consider a general target with an arbitrary radar cross section (amplitude pattern) in the following formulation (see [2]). However, for notational simplicity, we absorb this amplitude pattern in the radar amplitude pattern.

SAR data [3] [1] , one obtains the following SAR signal:

$$a_b(x_n, y_n - u, \omega) \ \exp\left[j2k\sqrt{x_n^2 + (y_n - u)^2}\right]. \tag{7}$$

Moreover, the bistatic SAR data yields the following spatial frequency reconstruction:

$$F_b(k_x, k_y) = A_b(k_u, \omega) \ \exp(jk_x x_n + jk_y y_n), \tag{8}$$

where

$$A_b[2k\sin\theta_n(u), \omega] = a_b(x_n, y_n - u, \omega), \tag{9}$$

and (k_x, k_y) are related to (k_u, ω) via (6). The spatial domain bistatic SAR image $f_b(x, y)$ is obtained via the two-dimensional inverse Fourier transform of $F_b(k_x, k_y)$.

The two radars are considered to be fully calibrated if

$$a_b(x, y - u, \omega) = a_m(x, y - u, \omega).$$

In this case, the two monopulse SAR images of stationary targets are also identical, i.e.,

$$F_b(k_x, k_y) = F_m(k_x, k_y),$$

and, thus, the difference image is a reliable statistic for moving target detection. This, however, is never achieved in practice.

In a practical monopulse SAR system, the two monostatic and bistatic radar amplitude patterns are not the same. This difference can be modeled as

$$a_b(x, y - u, \omega) = a_m(x, y - u, \omega) \ \left[1 + e(x, y - u, \omega)\right], \tag{10}$$

where $e(x, y - u, \omega)$ is an unknown pattern which contains a phase function as well as a gain (magnitude) function. Using the expression for the bistatic amplitude pattern in (10) and the Fourier properties of the SAR's AM-PM signal in [2, Appendix], the bistatic SAR reconstruction in the spatial frequency domain (see (8)) becomes

$$F_b(k_x, k_y) = A_m(k_u, \omega) \ \left[1 + E(k_u, \omega)\right] \ \exp(jk_x x_n + jk_y y_n), \tag{11}$$

---

[3]   This phase compensation approximately removes a shift in the bistatic data with respect to the monostatic data; the shift is related to the distance of the two radars in the along track domain [1]. Any residual error in this processing also corresponds to a shift operation which can be viewed as a component of the unknown impulse response $h(x, y)$. Thus, this additional shift error is already incorporated in the general model of (13); i.e., $h(x, y)$ contains a smearing component due to the calibration gain and phase errors, and a shift component due to the residual shift error.

where

$$E[2k \sin \theta_n(u), \omega] = e(x_n, y_n - u, \omega), \tag{12}$$

and (k_x, k_y) are related to (k_u, ω) via (6).

Comparing (5) and (11), we can write the following:

$$F_b(k_x, k_y) = H(k_x, k_y) \ F_m(k_x, k_y)$$
$$f_b(x, y) = f_m(x, y) \ ** \ h(x, y) \tag{13}$$

where

$$H(k_x, k_y) = 1 + E(k_u, \omega), \tag{14}$$

represents the transfer function of a linear shift-invariant system; $h(x, y)$, the impulse response, is the two-dimensional inverse Fourier transform of $H(k_x, k_y)$, and $**$ denotes two-dimensional convolution in the spatial domain.

Equations (13) and (14) indicate that the bistatic SAR image is a filtered (smeared and/or shifted) version of the monostatic SAR image; the transfer function of the filter $H(k_x, k_y)$ is related to the phase and gain differences of the two uncalibrated radars. This can result in gain and phase differences between the monostatic and bistatic SAR images of stationary targets. In this case, the difference image is not a reliable statistic for moving target detection.

Figure 1d shows the bistatic SAR image for a case involving uncalibrated radars. For this example, we use 35 nonzero coefficients ($N_x = 5$ pixels by $N_y = 7$ pixels) for the filter $h(x, y)$. The complex coefficients of $1 - h(x, y)$ are generated with a random number generator with a gain of approximately .2 and a uniform random phase. Figure 1e is the difference image. Note that the difference image for this case contains a significant contribution from the stationary targets (foliage) as well as the moving targets.

4. Signal Subspace Processing for Uncalibrated Radars

4a. Algorithm

The two-dimensional system model and the resultant effect which are described for a monopulse SAR system in the previous section, are similar to the clutter cancellation problem in one-dimensional active/passive imaging problems with monopulse radar and shipboard infrared search [3]-[6]. For these applications, the use of adaptive filtering methods has been suggested [7]. One may consider a two-dimensional version of such algorithms for the problem of uncalibrated radars in the two-dimensional monopulse SAR systems. However, the implementation of the adaptive filtering approach requires inversion of a

5

very large covariance matrix for each subpatch of the target scene, or a recursive (itera-tive) gradient descent solution [6]-[7]. Another version of the algorithm requires a priori knowledge of certain clutter parameters which should remain unchanged in the SAR scene [6]. Unfortunately, this is not an appropriate assumption in a high-resolution SAR image.

Equations (13)-(14) indicate that while $f_b(x, y)$ is a smeared version of $f_m(x, y)$, how-ever, the bistatic SAR image belongs to the linear signal subspace of the monostatic SAR image and its shifted versions in the case of *stationary targets*. Thus, one can first obtain the projection of $f_b(x, y)$ into this signal subspace, call it $\hat{f}_b(x, y)$. Then, the difference of this signal subspace projection $\hat{f}_b(x, y)$ and the bistatic SAR image $f_b(x, y)$ should provide a reliable statistic for moving target detection.

Let $\psi_\ell(x, y)$, $\ell = 0, 1, 2, \ldots, N - 1$, be the orthogonal basis functions which represent the above-mentioned signal subspace

$$\Psi \equiv \left[\, \psi_\ell(x, y); \; \ell = 0, 1, 2, \ldots, N - 1 \, \right].$$

To generate this signal subspace, one can use Gram-Schmidt, modified Gram-Schmidt, Householder or Givens orthogonalization procedure [8]-[10]. The choice depends on the type of digital signal processing software package which the user utilizes, and the accuracy of a given orthogonalization method in that software package.

The size of the subspace, i.e., N, depends on the user's a priori knowledge of the number of the nonzero coefficients in the discrete model of the impulse response $h(x, y)$. For instance, if the discrete $h(x, y)$ contains (N_x, N_y) non-zero pixels, then we should select $N = N_x N_y$. (A similar assignment/model for $h(x, y)$ is used in the adaptive filtering methods [6]-[7].) In practice, the exact value of $N_x N_y$ is not known. In this case, an estimate should be used based on the degree of gain and phase differences (calibration erros) between the two radars. We should emphasize that the algorithm is not sensitive to the fact that N might be chosen to be different from $N_x N_y$ (as long as the difference is not very large). For instance, in the example which we will examine, $N_x N_y = 5 \times 7 = 35$, while we use $N = 9$ for the number of the basis functions.

The projection of the bistatic image $f_b(x, y)$ into the basis function $\psi_\ell(x, y)$, which is identified by the series coefficient b_ℓ ($\ell = 0, 1, 2, \ldots, N - 1$), is found via the following:

$$\begin{aligned} b_\ell &\equiv \; < f_b \, , \, \psi_\ell \, > \\ &= \int_x \int_y f_b(x, y) \, \psi_\ell^*(x, y) \; dx dy \end{aligned} \tag{15}$$

where ψ^* is the complex conjugate of ψ. (For a discrete reconstructed image, the above double integral in the (x, y) domain is replaced with a double discrete sum over the available (x, y) pixels.)

6

The projection of the bistatic image into the signal subspace Ψ is defined via

$$\hat{f}_b(x,y) \equiv \sum_{\ell=0}^{N-1} b_\ell \, \psi_\ell(x,y). \qquad (16)$$

The signal subspace difference image, i.e., the statistic for moving target detection is constructed via

$$\hat{f}_d(x,y) \equiv f_b(x,y) - \hat{f}_b(x,y). \qquad (17)$$

Consider the monopulse SAR problem which was cited earlier. We use a signal subspace with size $N = 9$ which is constructed from $f_m(x,y)$ and its eight adjacent shifted versions. Figure 1f is the subspace difference image $\hat{f}_d(x,y)$ when the radars are fully calibrated. Note that this image resembles the difference image of the calibrated radars in Figure 1c. Now, consider the uncalibrated bistatic radar data of Figure 1d which corresponds to $N_x N_y = 35$ ($N_x = 5$ and $N_y = 7$) nonzero coefficients for the impulse response $h(x,y)$. (Note that the size of the subspace, i.e., $N = 9$, is less than the number of nonzero coefficients of $h(x,y)$.) Figure 1g shows the subspace difference image $\hat{f}_d(x,y)$ for the uncalibrated radars. Note that this shows a significant improvement over the difference image of uncalibrated radar data in Figure 1e. When we increase the signal subspace to 35 (i.e., $f_m(x,y)$ and its 34 adjacent shift versions), we obtain a subspace difference image for uncalibrated radars which is almost identical to the subspace difference image for calibrated radars in Figure 1f.

4b. Implementation and Computational Efficiency

Provided that the calibration error function $e(x, y - u, \omega)$ is inavriant of the target's coordinates, then the subspace processing can be applied in one step to the entire SAR scene. The same is impractical for the adaptive filtering approach [6]-[7] due to the enormously large size of the covariance matrix which has to be inverted. (The size of the SAR scene which is considered in Figures 1a-g, is 30 pixels by 386 pixels which is a subpatch of a larger 256 pixels by 1024 pixels SAR image. In this case, it is even impractical to implement the adaptive filtering approach for the 30 pixels by 386 pixels SAR subpatch on a regular computer.) When the error function cannot be modeled to be invariant of the target's coordinates, then the SAR image has to be divided into subpatches over which the error function does not vary significantly (which implies that $h(x,y)$ approximately remains the same in that subpatch.) The subspace algorithm can then be applied to each subpatch.

We have implemented the subspace algorithm using Matlab on a time-share computer at our school. For the example of Figures 1a-g, the CPU time for creating the signal

7

subspace Ψ is 5.1 sec; the CPU time to construct b_ℓ, $\ell = 0, 1, 2, \ldots, N - 1$, and $\hat{f}_b(x, y)$ from (15)-(16) is 1 sec.

4c. Stability and Noise Effect

Both the adaptive filtering method in [6] and the signal subspace projection of (15)-(16) seek the same *minimum error energy* solution for the bistatic SAR reconstruction $f_b(x, y)$ in the linear subspace of the monostatic SAR reconstruction $f_m(x, y)$ and its shifted versions. In the adaptive filtering approach, a solution for the impulse response $h(x, y)$ from the knowledge of $f_m(x, y)$ and $f_b(x, y)$, [4] call it $\hat{h}(x, y)$, is obtained via minimizing the following error function:

$$\int_x \int_y \left[\, f_b(x, y) - f_m(x, y) \, ** \, \hat{h}(x, y) \, \right]^2 \, dx dy. \tag{18}$$

For the available discrete data, $h(x, y)$ is modeled by, e.g., N nonzero coefficients (N_x pixels by N_y pixels, where $N = N_x N_y$). The resultant solution is then used to estimate $f_b(x, y)$ via the following:

$$\hat{f}_b(x, y) = f_m(x, y) \, ** \, \hat{h}(x, y). \tag{19}$$

In the proposed signal subspace method, the object is not to solve the deconvolution problem (i.e., to estimate the impulse response $h(x, y)$) which is computationally intensive, and may yield unstable results (depending on the condition of the covariance matrix). The signal subspace approach provides a direct solution for $\hat{f}_b(x, y)$ without the need to solve the deconvolution problem. Furthermore, to reduce additive noise effect, the user can discard the basis functions which possess relatively weak eigenvalues. (This step can be easily incorporated during the generation of the basis functions.)

Figure 2a-g show the same signals as in Figures 1a-g when the data are corrupted with a complex normal additive noise; the variance of the noise is chosen such that the signal-to-noise ratio (SNR) in Figures 2a, 2b and 2d is 4.5 dB; the additive white noise in these three images are uncorrelated (generated separately). (None of the basis functions are discarded for this example.) The moving targets' SAR signatures are prominent in the subspace difference images for calibrated (Figure 2f) and uncalibrated radars (Figure 2g) as well as the difference image for calibrated radars (Figure 2c). The difference image of uncalibrated radars (Figure 2e) shows the worst performance for moving target detection.

---

[4] This operation is called *deconvolution*.

8

Note that the K-L transform of the white noise's autocorrelation, i.e., the delta function, has a uniform eigenvalue distribution in Ψ and its complement Ψ^c [11]. Thus, the portion of the white noise in the measurement of $f_b(x,y)$ which falls in Ψ is filtered in the signal subspace difference processing. However, if a moving target's SAR signature does not belong to the subspace of the clutter (i.e., they are orthogonal), then the subspace difference processing will not attenuate the moving target's SAR signature.

5. Future Plans

We plan to continue our theoretical investigation on developing more compact signal subspaces of the monostatic SAR image $f_m(x,y)$ and its shifted versions for representing the bistatic image $f_b(x,y)$. This depends on the nature of the error function $E(k_u,\omega)$ which are encountered in practice. For instance, in some radar systems, the error function may take on the following form:

$$E(k_u,\omega) = \omega \ E_0(k_u) \ \exp[j\omega \ \phi_0(k_u)];$$

the above two-dimensional signal represents aspect angle-dependent phase and gain errors that linearly vary with the radar frequency. We also plan to investigate the implications of these error functions in estimating the motion parameters of a moving target in the SAR scene.

Moreover, our simulated results on signal subspace processing show sufficient promise that we believe the algorithm can now be tested on realistic monopulse SAR data. This study would reveal the nature of realistic calibration errors which could guide us in developing more compact and efficient signal subspace processing algorithms.

REFERENCES

1. M. Soumekh, "Moving target detection in foliage using along track monopulse synthetic aperture radar imaging," accepted for publication in *IEEE Transactions on Image Processing.*

2. M. Soumekh, "Reconnaissance with ultra wideband UHF synthetic aperture radar," *IEEE Signal Processing Magazine,* July 1995.

3. B. Cantrell, "A short-pulse area MTI," NRL Report 8162, September 1977.

4. A. Leonov and K. Fomichev, *Monopulse Radar,* Translated by W. Barton, Artech House 1986.

5. S. Sherman, *Monopulse Principles and Techniques,* Artech House, 1984.

6. M. Hartless and J. Barry, "Shipboard infrared search and track," Final Report of Contract N66001-94-C-6001, NCCOSC, December 1994.

7. B. Widrow, *Adaptive Signal Processing,* Englewood Cliffs, NJ: Prentice Hall, 1985.

8. G. Strang, *Linear Algebra and Its Applications,* pp. 276-282, New York: Academic Press, 1976.

9. A. Householder, *The Theory of Matrices in Numerical Analysis,* Waltham, MA: Ginn-Blaisdell, 1964.

10. G. Forsythe, M. Malcom and C. Moler, *Computer Methods for Mathematical Computations,* Englewood Cliffs, NJ: Prentice Hall, 1977.

11. H. Van Trees, *Detection, Estimation, and Modulation Theory,* vol. I, pp. 196-197, New York: Wiley, 1968.
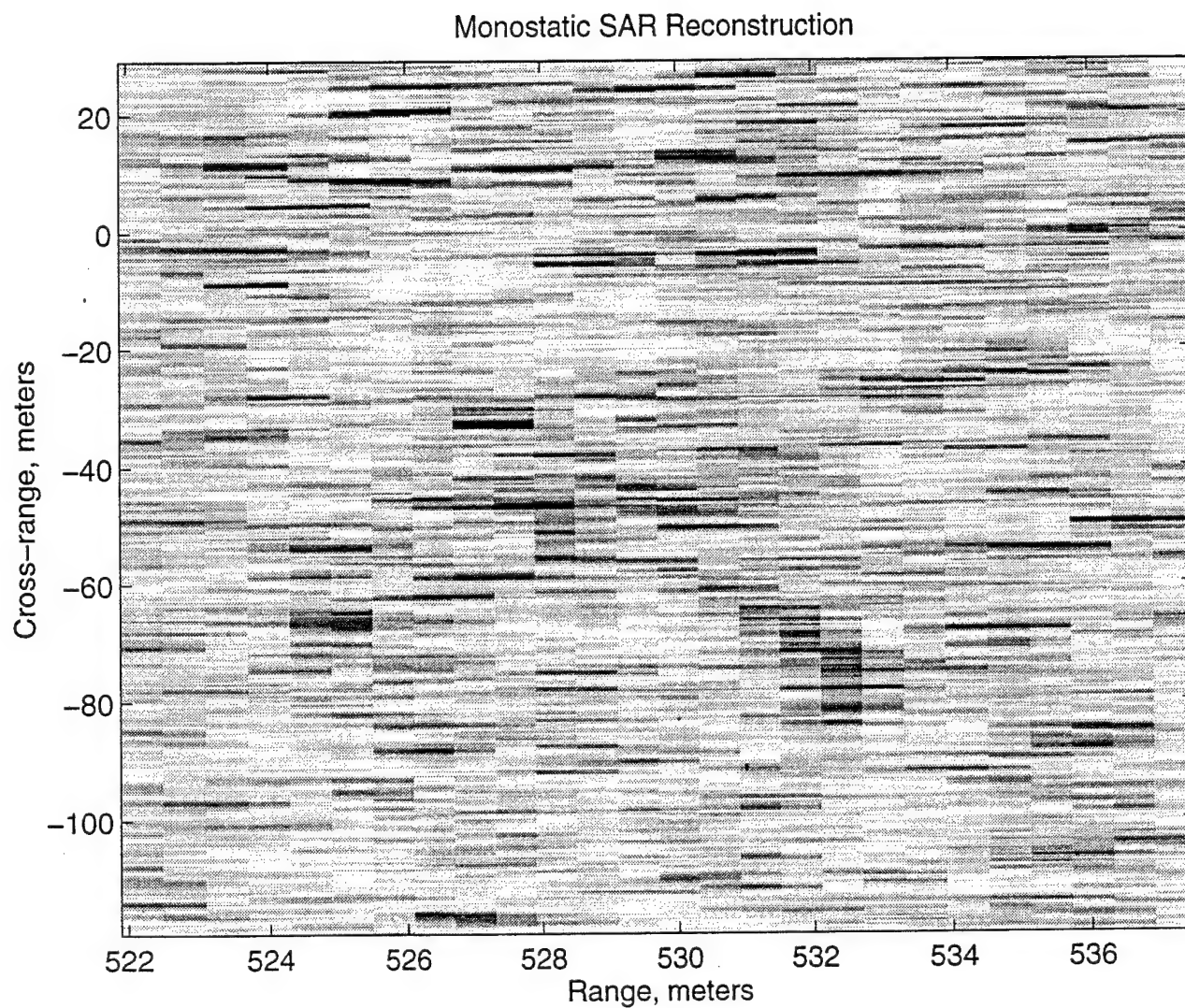
Figure 1a. Monostatic SAR reconstruction.
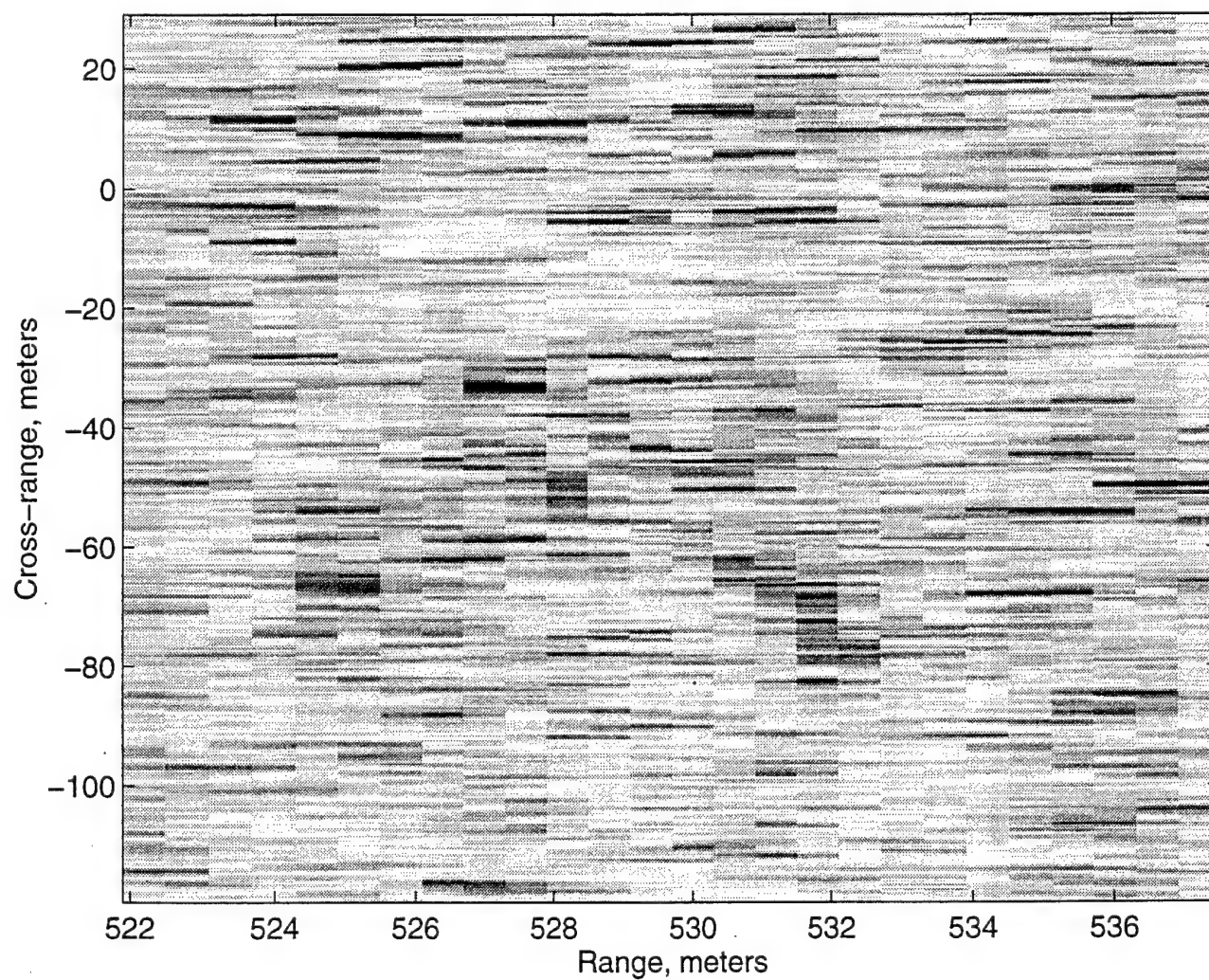
Figure 1b. Bistatic SAR reconstruction (calibrated radars).

Difference Image (calibrated radars)
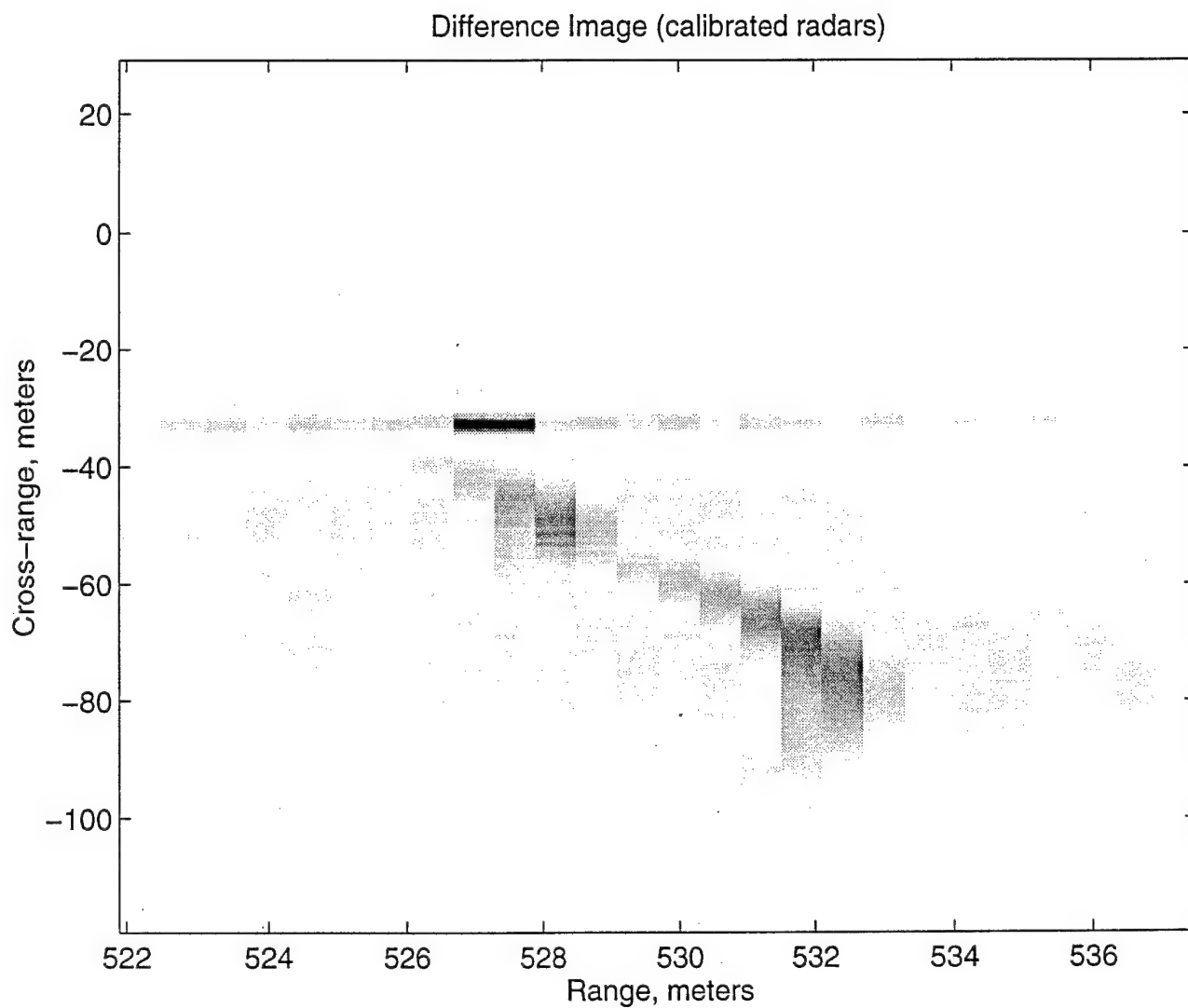
Figure 1c. Difference image (calibrated radars).

Bistatic SAR Reconstruction (uncalibrated radars)
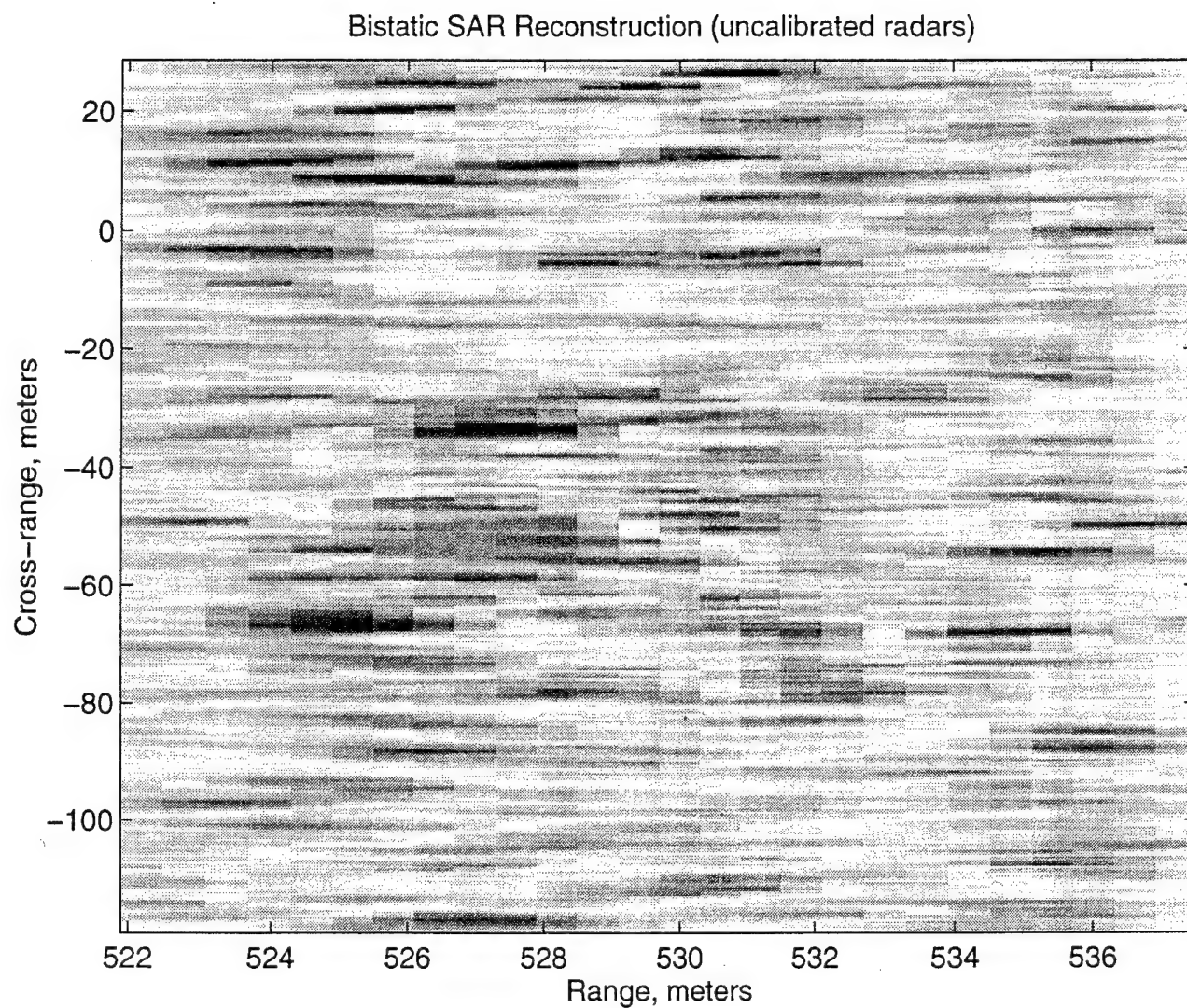
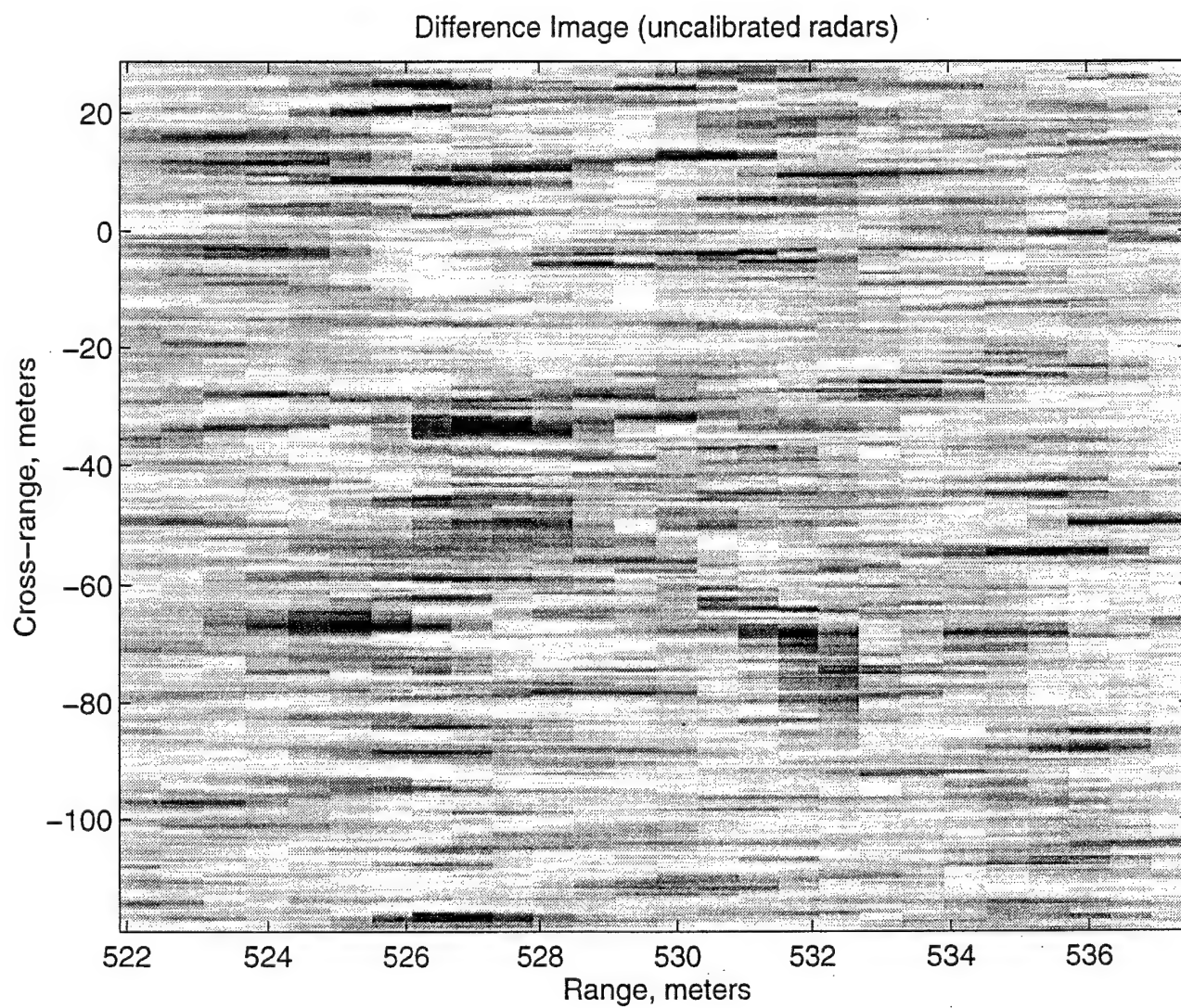Figure 1d. Bistatic SAR reconstruction (uncalibrated radars).

Figure 1e. Difference image (uncalibrated radars).

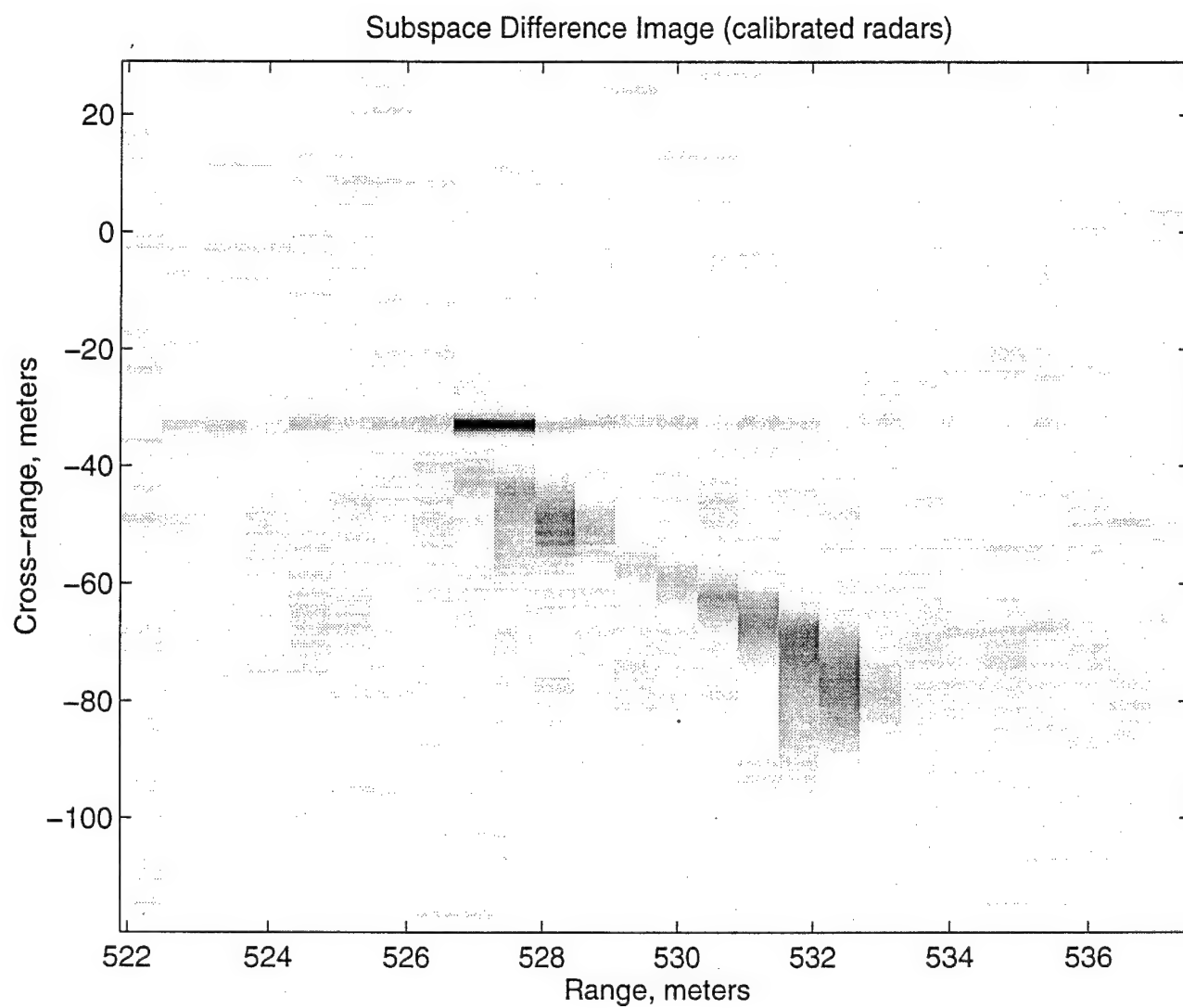Subspace Difference Image (calibrated radars)
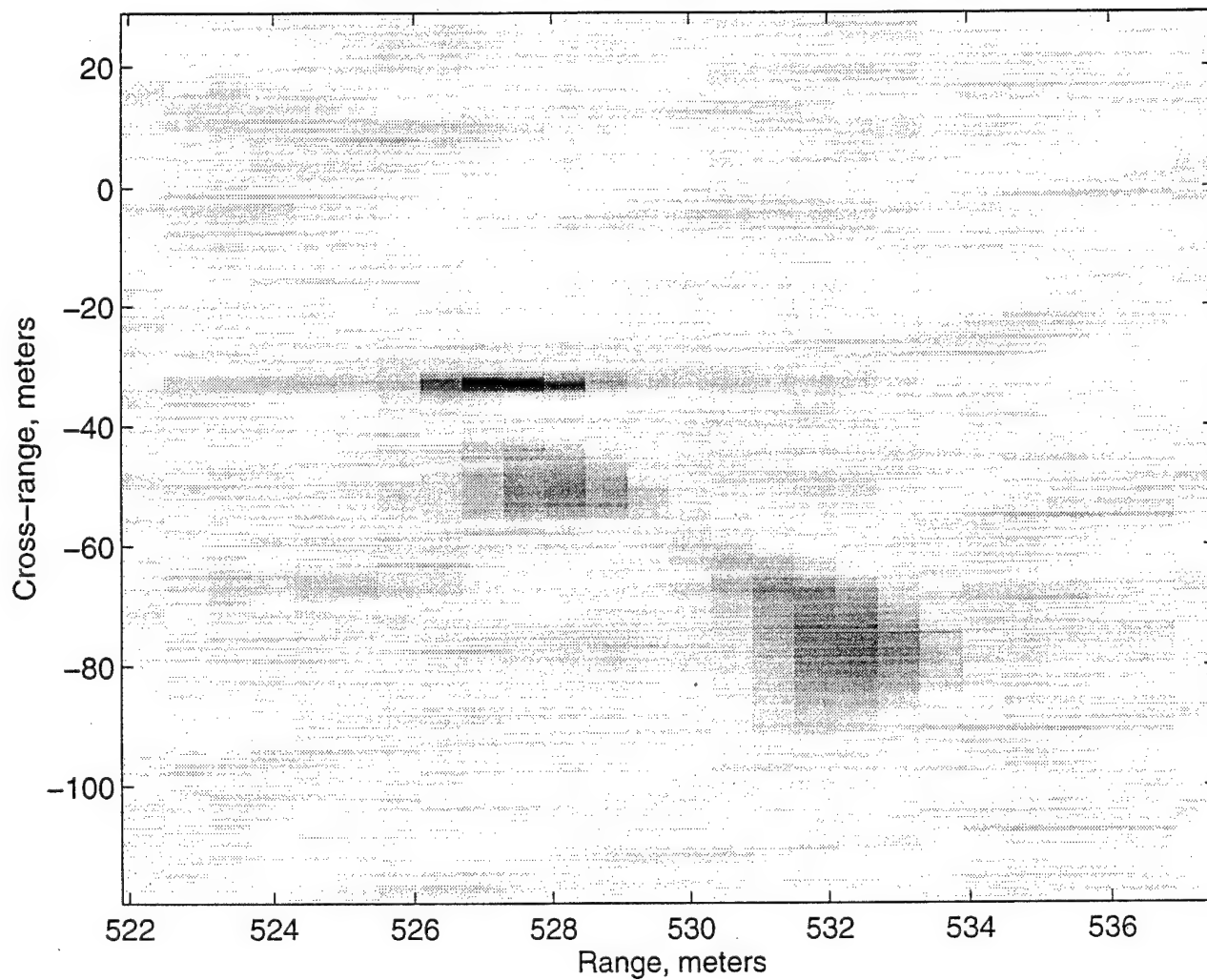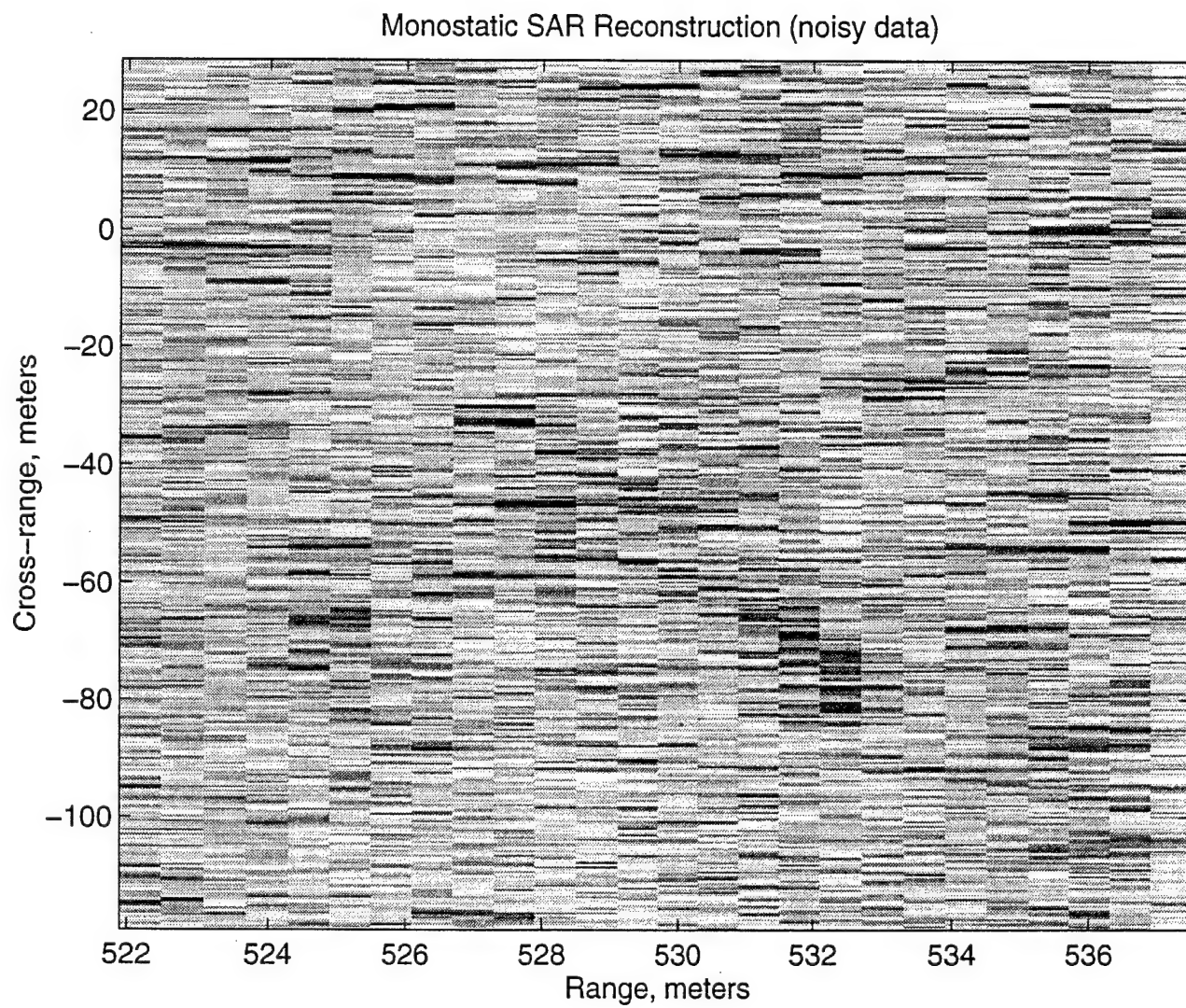
Figure 1f. Subspace difference image (calibrated radars).

Subspace Difference Image (uncalibrated radars)

Figure 1g. Subspace difference image (uncalibrated radars).

Figure 2a. Monostatic SAR reconstruction (noisy data).

Bistatic SAR Reconstruction (calibrated radars; noisy data)
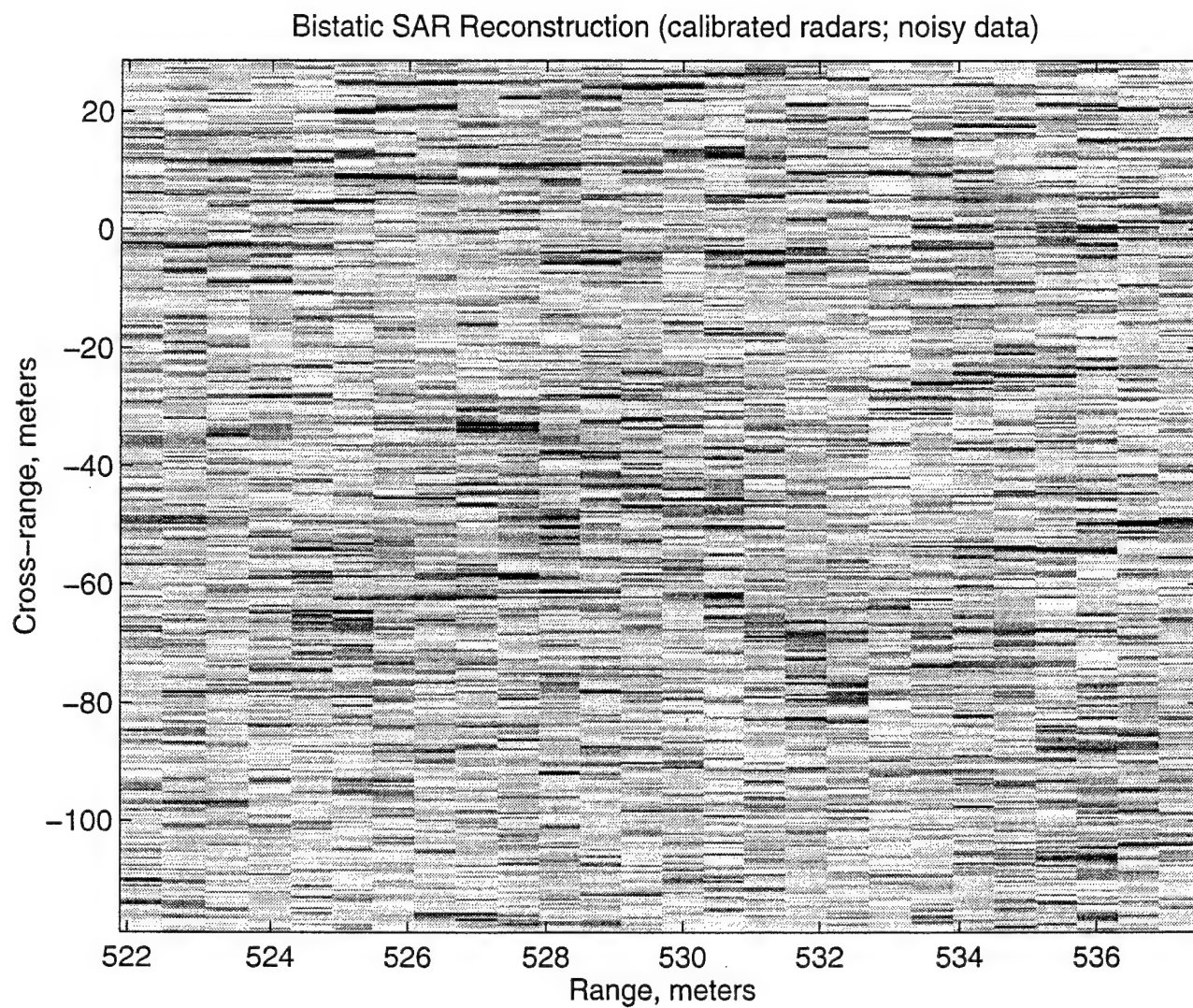
Figure 2b. Bistatic SAR reconstruction (calibrated radars; noisy data).

Difference Image (calibrated radars; noisy data)
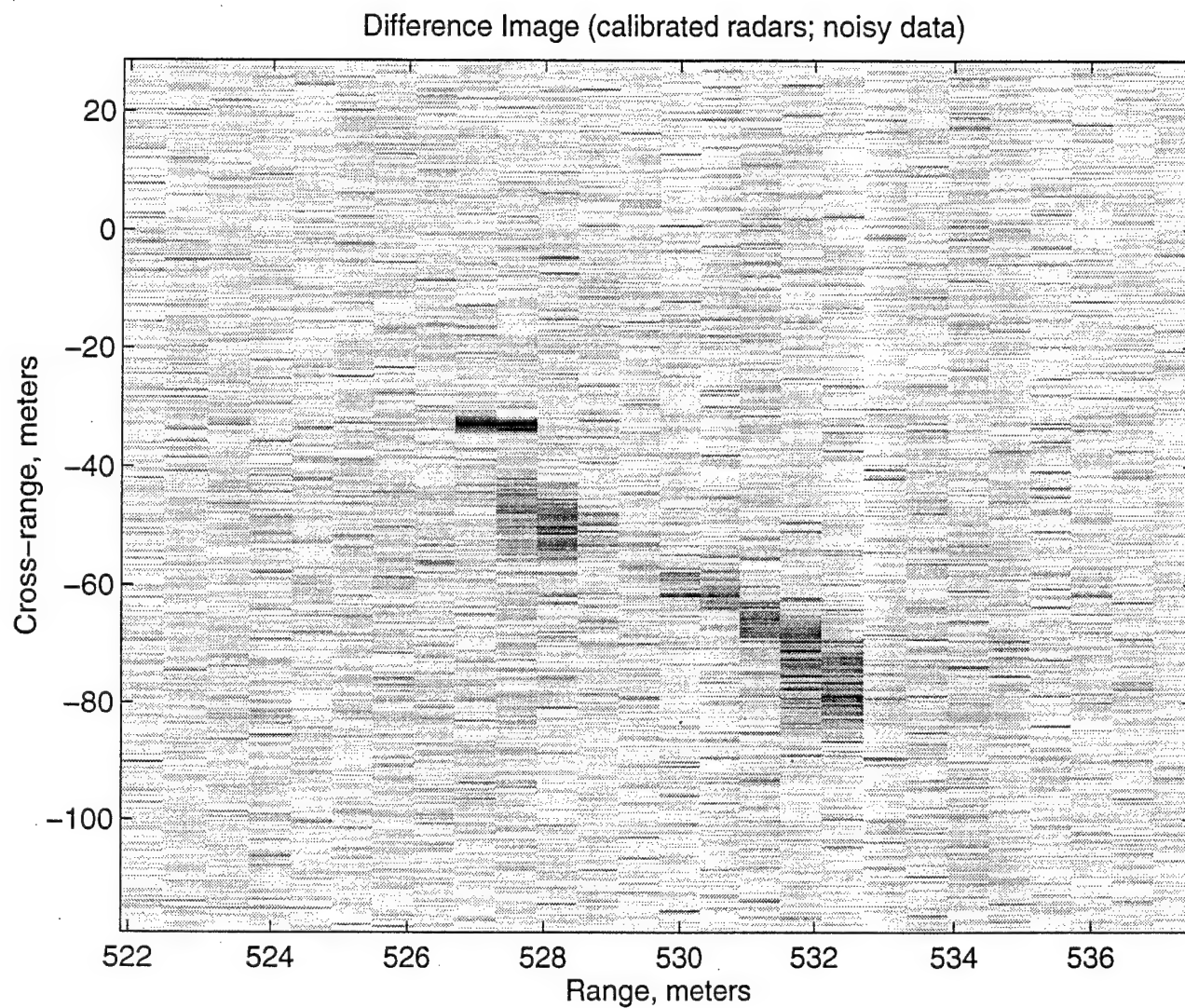
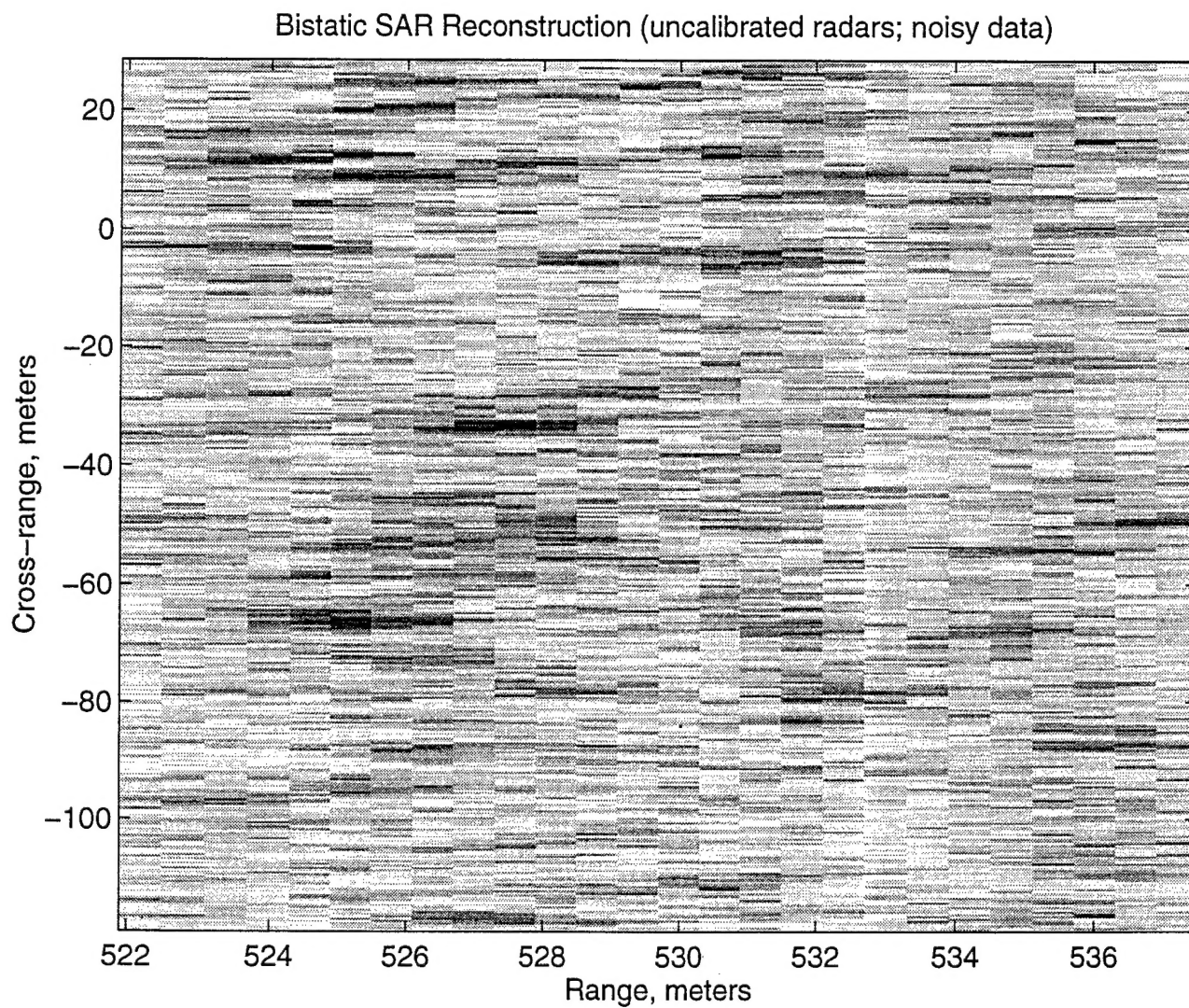Figure 2c. Difference image (calibrated radars; noisy data).

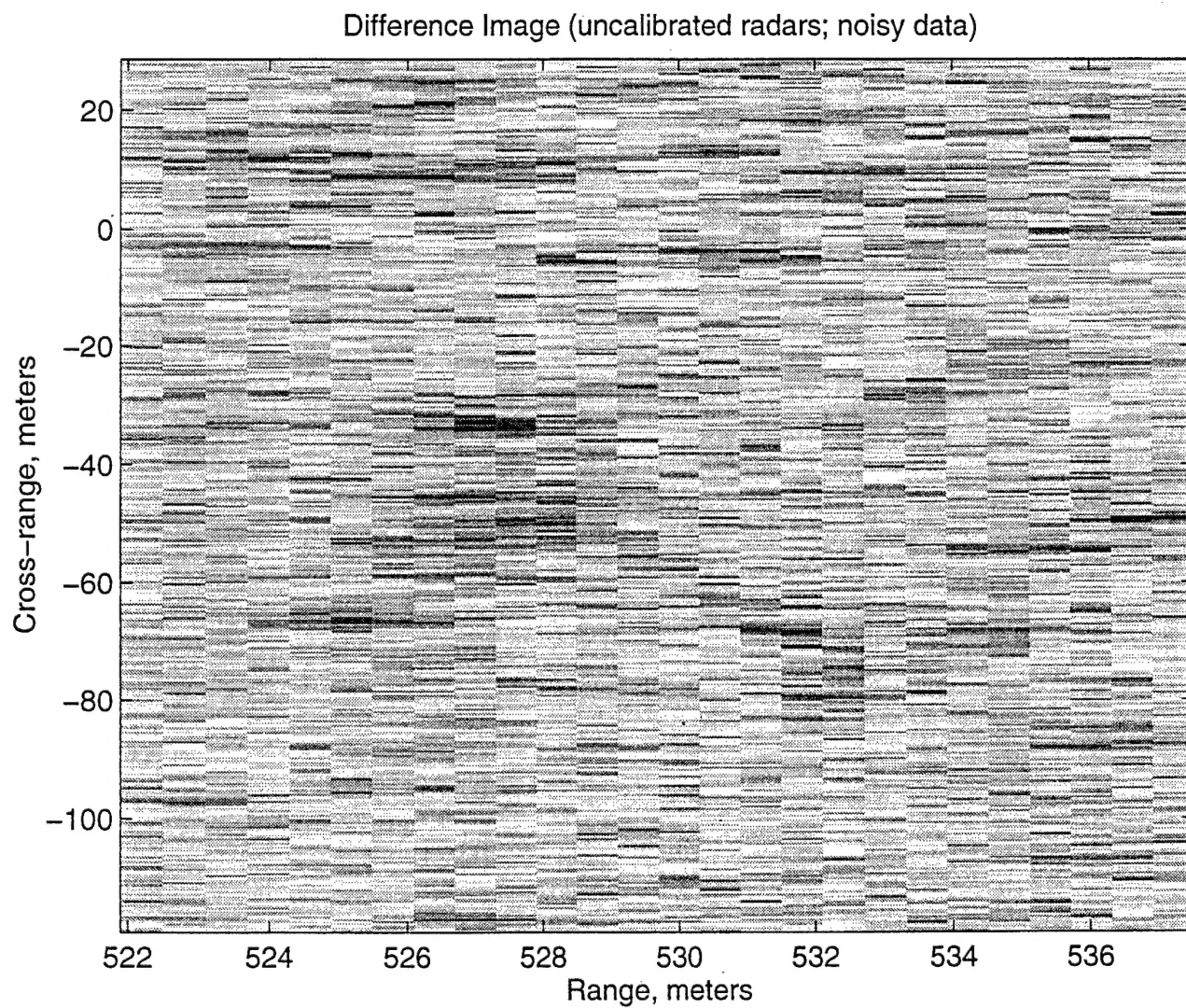Figure 2d. Bistatic SAR reconstruction (uncalibrated radars; noisy data).

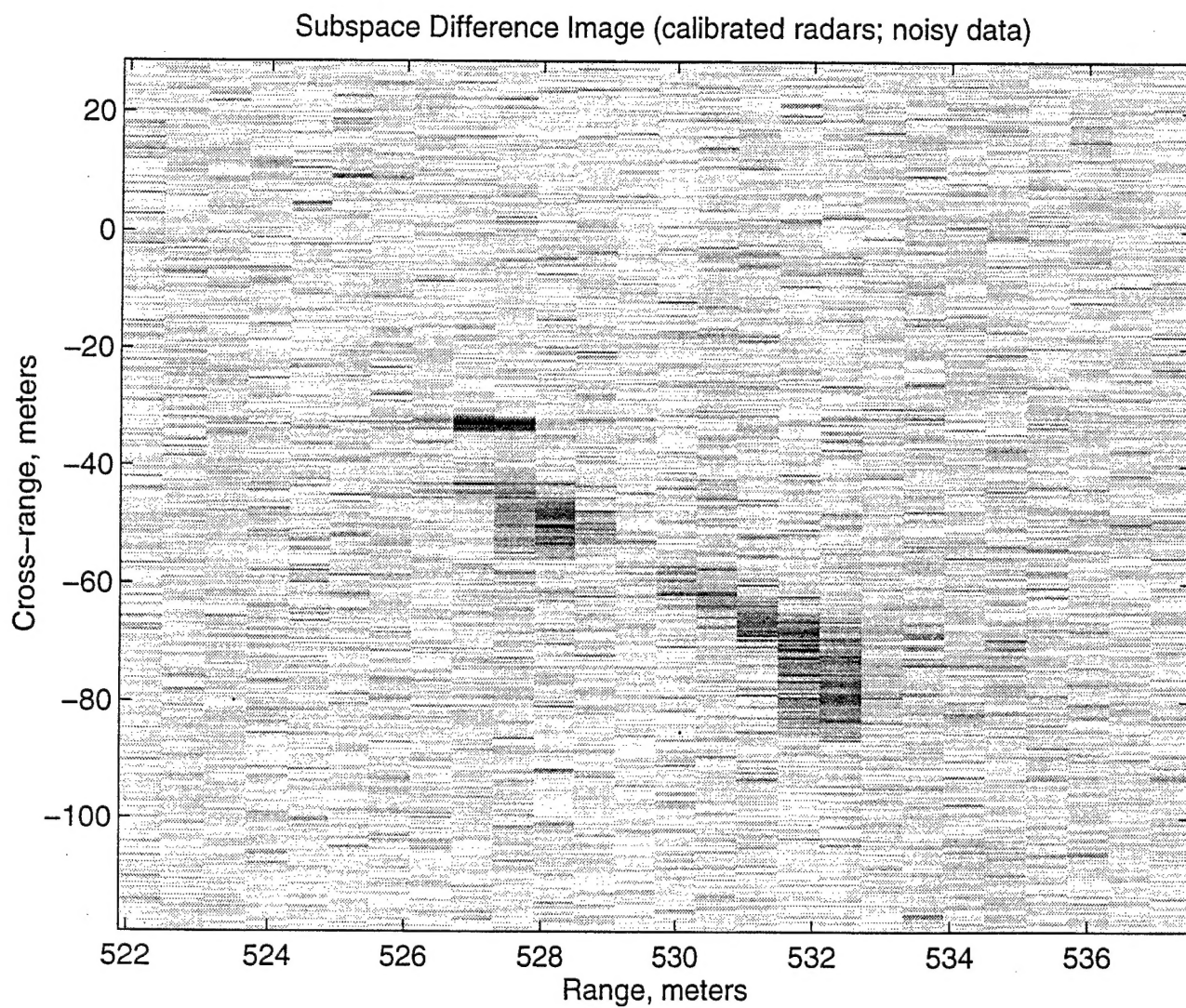Figure 2e. Difference image (uncalibrated radars; noisy data).

Subspace Difference Image (calibrated radars; noisy data)

Figure 2f. Subpspace difference image (calibrated radars; noisy data).

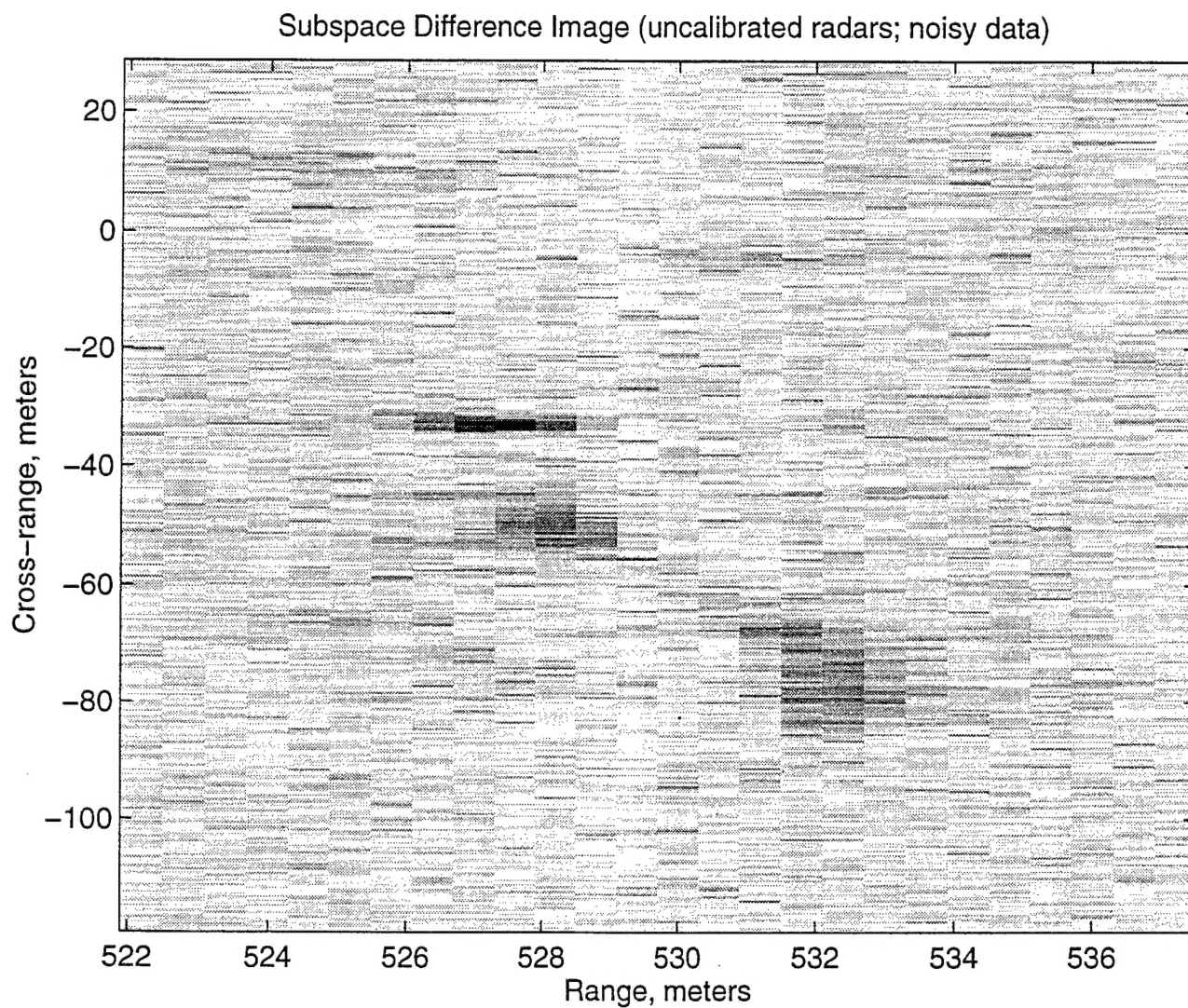Subspace Difference Image (uncalibrated radars; noisy data)

Figure 2g. Subspace difference image (uncalibrated radars; noisy data).